PAPER

Design and performance evaluation of microstrip fractal multiband patch antenna for wireless communication applications

To cite this article: Sudhir A Kadam and Dadaso D Mohite 2025 *Eng. Res. Express* **7** 035307

Engineering Research Express

RECEIVED
1 May 2025

REVISED
29 June 2025

ACCEPTED FOR PUBLICATION
30 June 2025

PUBLISHED
8 July 2025

PAPER

Design and performance evaluation of microstrip fractal multiband patch antenna for wireless communication applications

Sudhir A Kadam and Dadaso D Mohite*

Bharati Vidyapeeth (Deemed to be University) College of Engineering, Pune-411043, India
* Author to whom any correspondence should be addressed.

E-mail: dadasomohite@gmail.com

Keywords: fractal multiband antenna, microstrip patch antenna, wireless communication, dielectric substrates, impedance matching, VSWR

Abstract

The rapid evolution of wireless communication technologies—particularly in the S-band and C-band frequencies used for WiMAX and 5G New Radio (NR) sub-6 GHz applications—has driven the need for compact, high-performance, and multiband antenna solutions capable of wideband and multi-frequency operation. This paper presents the design and performance evaluation of a novel Microstrip Fractal Multiband Patch Antenna (MPA) tailored for such wireless communication systems. The antenna utilizes fractal geometry to overcome the limitations of conventional microstrip patch designs, achieving enhanced bandwidth, multi-resonant behavior, and a reduced physical footprint. The incorporation of self-similar fractal patterns within a square-cut, multi-hole patch structure enables efficient dual-band operation across distinct frequency ranges. Simulation results, obtained using HFSS software, demonstrate excellent impedance matching, with a Voltage Standing Wave Ratio (VSWR) below 2 and a reflection coefficient below −10 dB over the S-band (2.3244 GHz–3.7692 GHz) and C-band (5.0936 GHz–7.1104 GHz). Experimental validation using a Vector Network Analyzer closely aligns with simulation data, confirming consistent and reliable performance. The antenna exhibits a bi-directional radiation pattern, ideal for point-to-point communication, and is fabricated using a cost-effective FR-4 glass epoxy substrate with copper cladding, ensuring ease of production and scalability. The proposed design offers superior multiband functionality, compactness, and efficiency, meeting the growing demand for advanced antennas in next-generation wireless communication systems. The results affirm its potential for integration into applications such as WiMAX, 5G NR, and other emerging wireless technologies.

1. Introduction

The ever-expanding domain of wireless communication technologies necessitates the development of antennas with advanced capabilities, including compactness, multi-band operation, and enhanced performance metrics such as gain, bandwidth, and efficiency [1, 2]. Antennas serve as crucial components in modern communication systems, transmitting and receiving electromagnetic signals that form the backbone of technologies like mobile phones, personal digital assistants (PDAs), Wi-Fi, and advanced broadband communication [3, 4]. Among various types of antennas, microstrip patch antennas have gained widespread popularity due to their low profile, lightweight structure, and ease of integration into devices [5]. However, traditional Euclidean geometries used in patch antennas face significant challenges, including limited bandwidth, high Q-factor, and efficiency loss as antenna sizes are reduced [6]. To address these challenges, this research explores the potential of fractal geometries in designing microstrip antennas, offering compactness and multi-band capabilities while overcoming traditional limitations [7].

Fractal geometries have gained prominence in antenna design due to their unique self-similar and space-filling properties. Dual-band patch antennas, which utilize fractal geometries, are particularly suited for multi-band applications [8]. These antennas are designed by repeatedly creating fundamental geometric patterns, resulting in a structure that can resonate at multiple frequencies. The increased perimeter of the material enhances the total electrical length of the antenna without increasing its surface area or volume [9]. This property, combined with the space-filling nature of fractal geometries, enables dual-band patch antennas to operate efficiently at different frequency bands while maintaining a compact size. Their ability to repeat patterns across two or more scale levels makes them versatile and highly efficient for microwave and cellular communication systems applications [10].

This research introduces a novel approach to designing dual-band patch antennas that emphasizes compact dimensions, mechanical robustness, and space utilization. The proposed antennas exhibit excellent efficiency, gain, and multi-band performance by leveraging the self-similar properties of fractal geometries. Additionally, the antennas' compact design allows them to be adhered to surfaces, conserving space and making them suitable for applications such as satellite systems and other compact wireless devices. The study also includes a comparative analysis of different techniques—microstrip line feed, coaxial feed, aperture-coupled feed, and proximity-coupled feed. The fabrication of efficient and cost-effective antennas is another critical aspect of this research. The proposed fractal microstrip antennas are designed using the FR-4 glass epoxy substrate, a widely available and low-cost material with a dielectric constant (εr) of 4.4 and a thickness of 1.6 mm. This material choice ensures affordability without compromising performance. The compact dimensions and space-filling properties of the dual-band patch antenna make it highly space-efficient, as the same antenna can function effectively across various frequency bands. Additionally, the mechanical simplicity and robustness of the design eliminate the need for discrete components, further enhancing its practicality for real-world applications.

This research paper focuses on the design, development, and performance evaluation of microstrip fractal MPAs for S-band and C-band wireless communication applications. By leveraging the unique advantages of fractal geometries and dual-band patch designs, the paper demonstrates how these antennas overcome the limitations of conventional designs, such as limited bandwidth and efficiency loss. The inclusion of novel features, such as compact dimensions, space-filling properties, and improved feeding techniques, positions this research as a significant advancement in antenna technology. Validated through applications in WiMAX (2.6 GHz) and 5G NR sub-6 GHz bands, the proposed design offers a scalable, efficient, and innovative solution for next-generation wireless communication systems. The novelty of this research lies in the integration of a modified Sierpinski carpet fractal geometry with circular etchings, enabling multi-resonant behavior across dual bands in a compact form factor. The rotational symmetry and 46% iterative scale-down technique optimize bandwidth without increasing complexity.

2. Methodology

2.1. Patch antenna design and fractal development

The design and development of an MPA for S-band and C-band wireless communication applications involves a systematic approach that ensures optimal performance across the desired frequency ranges. Figure 1 depicts the systematic approach followed in the design, simulation, and fabrication of the proposed MPA. Each step in the process is outlined to ensure that the antenna meets the desired specifications for S-band and C-band wireless communication applications.

The design process for the proposed MPA begins with the development of a microstrip patch antenna, a widely used antenna types due to its simplicity and ease of fabrication [11]. The first step in this process is determining the geometric structure of the antenna, which is primarily driven by the frequency bands and the required performance parameters. The initial iteration is a square-cut patch antenna, which serves as the baseline design. This configuration helps to define the essential characteristics of the radiating element, such as its resonance frequency and radiation pattern. To enhance the antenna's performance, particularly its bandwidth and efficiency, the square-cut antenna is further modified into a square-cut multi-hole design. This modification involves the strategic introduction of circular holes in the patch, which helps in optimizing the antenna's multiband characteristics. These holes not only improve the bandwidth but also increase the antenna's ability to operate efficiently at multiple frequency bands, making it suitable for wireless communication systems that require coverage over different frequency ranges, such as the S-band and C-band [12].

Building on the initial design, the next step introduces a fractal antenna concept, which is known for its ability to reduce the physical size of the antenna while maintaining its electrical length, thus enhancing its multiband performance. The fractal antenna design is based on the previously established square-cut multi-hole patch, with the addition of self-similar geometric patterns that provide space-filling properties. These patterns enable the antenna to operate efficiently at multiple resonant frequencies within a compact size. The first iteration of the fractal antenna integrates these self-similar shapes into the design, thereby improving its

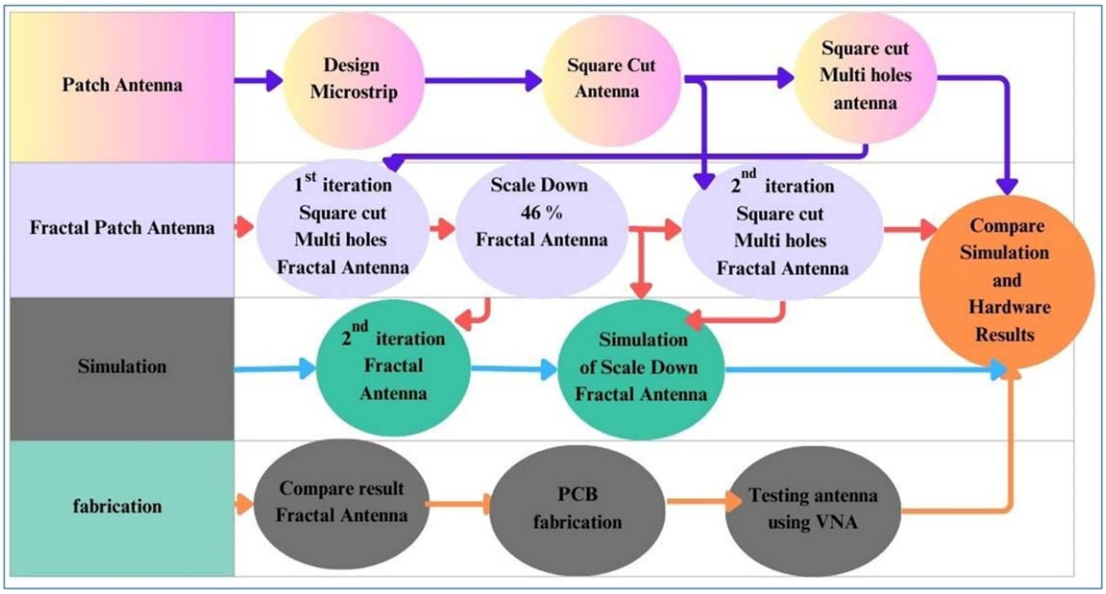

Figure 1. Antenna design and development process.

performance across the targeted frequency bands. To further optimize the antenna, a 46% scale-down of the fractal antenna is performed, resulting in a more compact version that retains the desirable multiband properties. This size reduction is crucial for applications where space constraints are important, such as in compact wireless devices or communication systems. Despite the size reduction, the antenna maintains its performance, ensuring that it can still effectively operate in both the S-band and C-band frequency ranges, making it ideal for modern wireless communication systems where size and performance are equally critical.

The antenna was fabricated on an FR-4 glass epoxy substrate using standard photolithography and etching processes. The designed pattern was transferred via UV exposure using a mask, followed by chemical development and etching to define the patch structure. An SMA connector was soldered onto the feed line for testing. These standard fabrication steps ensured precision in reproducing the simulated design.

3. Design and development of MPA

Developing a dual-band patch antenna involves iterative processes to design a self-similar structure. This approach allows the creation of smaller antenna elements while maintaining desirable features such as high efficiency and wide bandwidth. The self-similar geometry forms the foundation of the dual-band patch antenna, enabling it to achieve compactness without sacrificing performance. The ability to scale the geometry for different iterations contributes to its suitability for multiband wireless communication systems [13].

Two primary methods are employed for designing MPAs using fractal geometries. The first method leverages the space-filling properties of the fractal structure, which enables long electrical lengths to be compressed into smaller physical volumes. This significantly reduces the antenna size without diminishing its efficiency or bandwidth [14]. The second method involves utilizing the scaled geometry of self-similar fractals to design antennas that operate at different frequency bands [15]. These antennas exhibit similar physical structures across multiple bands, resulting in a uniform design that enhances versatility and performance in applications requiring multiband functionality [16]. The Modified Sierpinski Carpet Fractal Geometry is employed in the design of the antenna. This fractal pattern, characterized by self-similar, recursively repeating shapes, is known for its ability to create multiple resonant frequencies within a compact structure. The circular etchings within the fractal pattern enhance the antenna's ability to operate over multiple frequency bands, which is crucial for modern communication systems that require multiband capabilities. The use of this geometry ensures that the antenna retains a small physical size while maintaining high performance across these bands. Moreover, the self-similar hole patterns contribute to efficient space utilization, making the antenna suitable for compact and portable devices, where size and performance are both important considerations.

The design of the MPA process begins with creating a square patch antenna measuring 30 mm × 30 mm, which serves as the radiating element. This patch is placed on a rectangular FR-4 substrate with dimensions of 48 mm × 65 mm, a thickness of 1.53 mm, and a relative permittivity (εr) of 4.4. To optimize the bandwidth and enhance performance, the edges of the square patch are curved using an 18 mm radius cylinder centered at the

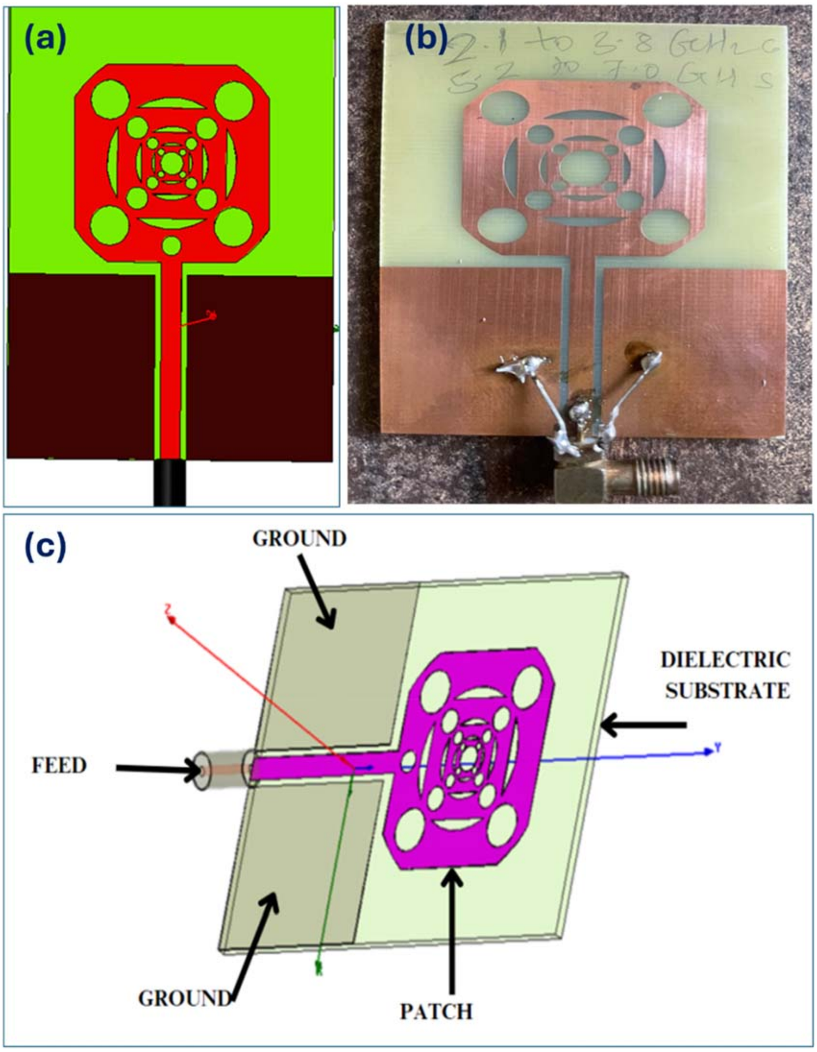

Figure 2. (a) Front view of multi-hole multiband microstrip fractal patch antenna (b) fabricated antenna; (c) schematic diagram with directions and dielectric substrate.

patch's centroid. This modification smoothens the current distribution, minimizes edge-related discontinuities, and thereby improves impedance matching and overall bandwidth performance. A cylindrical section, 10 mm long, is etched out at the center of the structure to fine-tune the design.

The core patch structure is scaled down to 46% of its original size for each subsequent iteration. Initially, a 45-degree rotation was considered during design trials, but it was not implemented in the final optimized structure as the required multiband response was achieved through scaling alone. Three such patches are connected to form the final antenna structure. A feed line, 3.1 mm wide, is attached to the patch. A level surface measuring 22.5 mm $\times$ 28 mm is maintained on both sides of the feed line to ensure proper functioning. The gap between the ground plane and the feed line is set at 0.95 mm, while the distance between the ground and the patch is maintained at 0.22 mm. The finalized design is shown in figure 2, highlighting the front view of the multi-hole multiband microstrip fractal patch antenna.

The antenna is fabricated using an FR-4 glass epoxy substrate, chosen for its affordability, ease of availability, and suitable dielectric properties. The copper conducting material is used for the radiating patch, ensuring excellent conductivity and minimal energy loss. This choice of materials provides a balance between cost-effectiveness and high-performance antenna fabrication, making it ideal for mass production in wireless communication applications.

The MPA features compact dimensions, making it ideal for space-constrained applications. Its small size allows it to easily adhere to surfaces, while its self-similarity enhances its aesthetic appeal and functional efficiency. Despite its reduced size, it offers high efficiency and improved gain compared to traditional antenna designs. The fractal geometry of the antenna enables effective space utilization, allowing the same design to operate across multiple frequency bands. This space-filling property makes the antenna highly versatile. Additionally, the antenna's design relies on the shape of the patch rather than discrete components, contributing

Table 1. Performance comparison between initial square patch and proposed fractal patch antenna.

Sr no.	Parameter	Initial square patch	Proposed fractal patch
1	Operational Bands	Single band (S-band only)	Dual band (S-band & C-band)
2	Bandwidth	~1.1 GHz	~3.7 GHz
3	Physical Size (Patch area)	30 mm × 30 mm	46% scaled fractal pattern
4	VSWR	Minimum ~1.8	Minimum ~1.4
5	Return Loss (dB)	~8.5 dB	>10 dB
6	Multiband Capability	No	Yes
7	Radiation Pattern	Uni-directional	Bi-directional

to its mechanical simplicity and robustness. This design approach enhances the adaptability of the antenna, allowing it to be easily attached to various surfaces, such as those in satellite applications.

Figure 2 illustrates the proposed Multi-hole Multiband Microstrip Fractal Patch Antenna. Figure 2(a) shows the simulated front view, highlighting the fractal patch design with multiple circular slots optimized for multiband performance. Figure 2(b) presents the fabricated antenna prototype on an FR4 substrate, including the SMA connector used for experimental testing. Figure 2(c) provides a 3D schematic of the antenna, detailing the feed line, patch structure, partial ground planes, and dielectric substrate along with coordinate axes, offering spatial context for analysis.

The proposed MPA was designed and tested to operate effectively in the S-band and C-band frequency ranges, catering to applications such as WiMAX (2.6 GHz) and 5G NR sub-6 GHz bands. The design's compact size, robust structure, and multiband capability make it suitable for integration into modern wireless communication systems. The validation process included performance testing in a controlled environment to ensure consistent results and optimal efficiency.

The uniqueness of the antenna lies in its hybrid geometry—combining fractal slotting with a multi-hole pattern and rotational symmetry—to achieve a wide operational range. Unlike traditional fractal patch antennas, this approach introduces geometric optimization that balances miniaturization with enhanced bandwidth, tailored for sub-6 GHz wireless communication.

3.1. Comparison with initial patch design

To evaluate the improvement achieved by the proposed fractal MPA, a performance comparison was conducted with the initial square-cut single-band patch antenna. Table 1 summarizes the key differences in design and output characteristics.

The results clearly show that the proposed design achieves multi-resonant performance, enhanced bandwidth, and compactness without compromising impedance matching. These improvements confirm the effectiveness of integrating self-similar fractal geometry and circular etchings for multiband wireless communication systems.

3.2. Iterative development of antenna design

The proposed antenna design was developed through a structured three-stage iterative process aimed at improving bandwidth, efficiency, and multiband functionality while preserving a compact form factor. The design evolution is illustrated in figure 3, highlighting the transformation from a basic patch structure to a refined fractal geometry optimized for dual-band performance.

In the first iteration, a square patch antenna with dimensions of 30 mm × 30 mm was implemented on an FR-4 substrate (65 mm × 48 mm, $\varepsilon_r = 4.4$, thickness = 1.53 mm). A central circular cut was introduced to perturb the current distribution, resulting in a single-band response with a return loss of approximately 8.5 dB. In the second iteration, symmetrical circular slots were added around the central region, and the inner geometry was scaled down by 46%. This modification increased the electrical path length and introduced multiple current loops, resulting in the appearance of additional resonant frequencies and the onset of multiband behavior. In the third iteration, a second 46% scale-down of the central geometry was embedded within the previous design, forming a self-similar fractal structure. This final configuration enhanced current distribution uniformity, reduced surface wave losses, and enabled dual-band operation across the S-band (2.32–3.76 GHz) and C-band (5.09–7.11 GHz), achieving a VSWR <1.4 and return loss >10 dB.

This iterative design approach underscores the effectiveness of fractal geometry and strategic scaling in achieving significant improvements in bandwidth, impedance matching, and multiband performance, confirming the suitability of the proposed antenna for applications such as WiMAX and 5G NR.

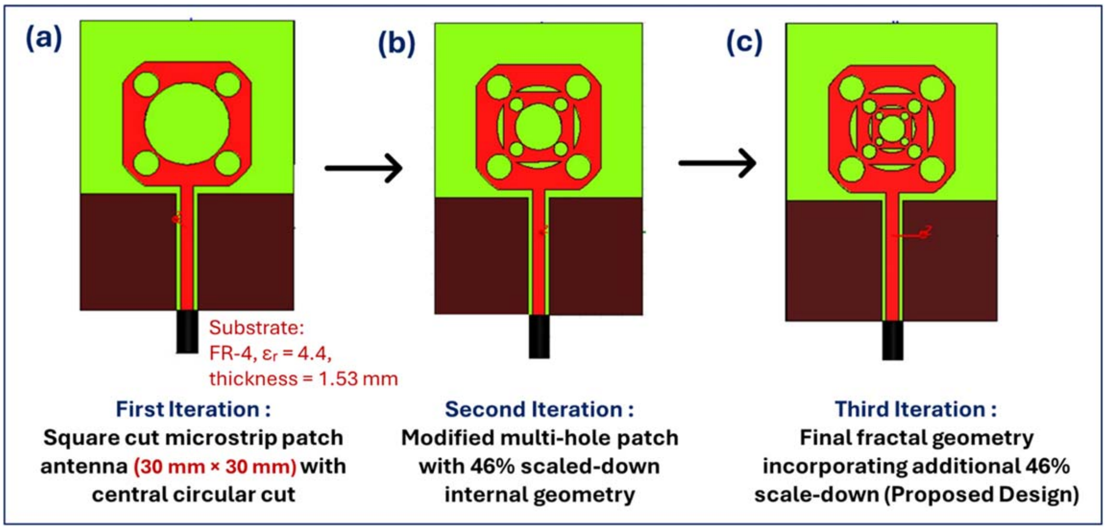

Figure 3. Iterative design evolution of the proposed fractal patch antenna: (a) circular-cut patch, (b) multi-hole patch with 46% scale-down, (c) Fractal geometry with additional 46% scale-down.

4. Simulated and experimental results

The proposed MPA design was analyzed and optimized using High-Frequency Structure Simulator (HFSS) software, a widely used tool for electromagnetic simulations. HFSS enabled precise modeling of the fractal geometry of the antenna, facilitating the evaluation of critical performance parameters such as return loss, gain, and bandwidth for the targeted S-band of 1.9 GHz to 3.8 GHz and C-band of 5.8 GHz to 7.9 GHz frequency ranges. The performance of the fabricated antenna was validated experimentally using a Vector Network Analyzer (VNA) at Falcon Electro-Tek Pvt Ltd, Koparkhairne, Mumbai. The VNA measurements confirmed the operational capabilities of the antenna in the S-band (2.2–3.0 GHz). However, the C-band performance (5.3–7.2 GHz) could not be validated experimentally due to the VNA's measurement limit of 3 GHz. Future work will include high-frequency validation using extended-range equipment. These results demonstrate excellent agreement between the simulated and experimental outcomes, underscoring the reliability and effectiveness of the proposed design for multiband wireless communication applications.

4.1. Voltage standing wave ratio (VSWR)

VSWR represents the efficiency of radiofrequency power transfer between the antenna and the transmission line, serving as a critical indicator of impedance matching [17]. A lower VSWR value, typically below 2, signifies optimal power transfer with minimal reflection losses. The simulated VSWR results for the proposed fractal MPA, depicted in figure 4(a), confirm its effective performance. Specifically, the simulation results demonstrate two distinct frequency bands of operation: the first band extends from 2.4263 GHz to 3.2018 GHz (S-band), providing a bandwidth of approximately 1.53 GHz, while the second band spans 5.3789 GHz to 7.2308 GHz (C-band), offering a bandwidth of approximately 2.17 GHz. This dual-band performance results in a total operating bandwidth of approximately 3.7 GHz, making the antenna highly suitable for S-band and C-band wireless communication applications.

The VSWR behavior, characterized by dips within the operational frequency ranges, is attributed to the optimized fractal geometry of the antenna, which enhances impedance matching and ensures efficient power transmission [18]. These results validate the robustness of the proposed design and underscore its potential for modern wireless systems, such as WiMAX (2.6 GHz) and 5G NR sub-6 GHz bands.

The experimental VSWR measurements for the fabricated antenna, as shown in figure 4(b), highlight its performance under real-world conditions by demonstrating its impedance-matching characteristics and resonant behavior across the operational frequency bands. The graph indicates a VSWR value below 2 at the resonant frequency of 2.2 GHz, confirming effective operation with minimal power reflection and optimal impedance matching. This result aligns closely with the simulated data, validating the antenna design and fabrication process. Also, the experimental measurements reveal multiple resonant frequencies, which can be attributed to the inclusion of the middle strip line in the antenna structure. This feature facilitates multi-resonant behavior, enabling the antenna to operate effectively over a broader range of frequencies. The deviations between simulated and measured VSWR are attributed to several practical factors. First, fabrication imperfections in etching accuracy and manual soldering of the SMA connector can introduce mismatch and

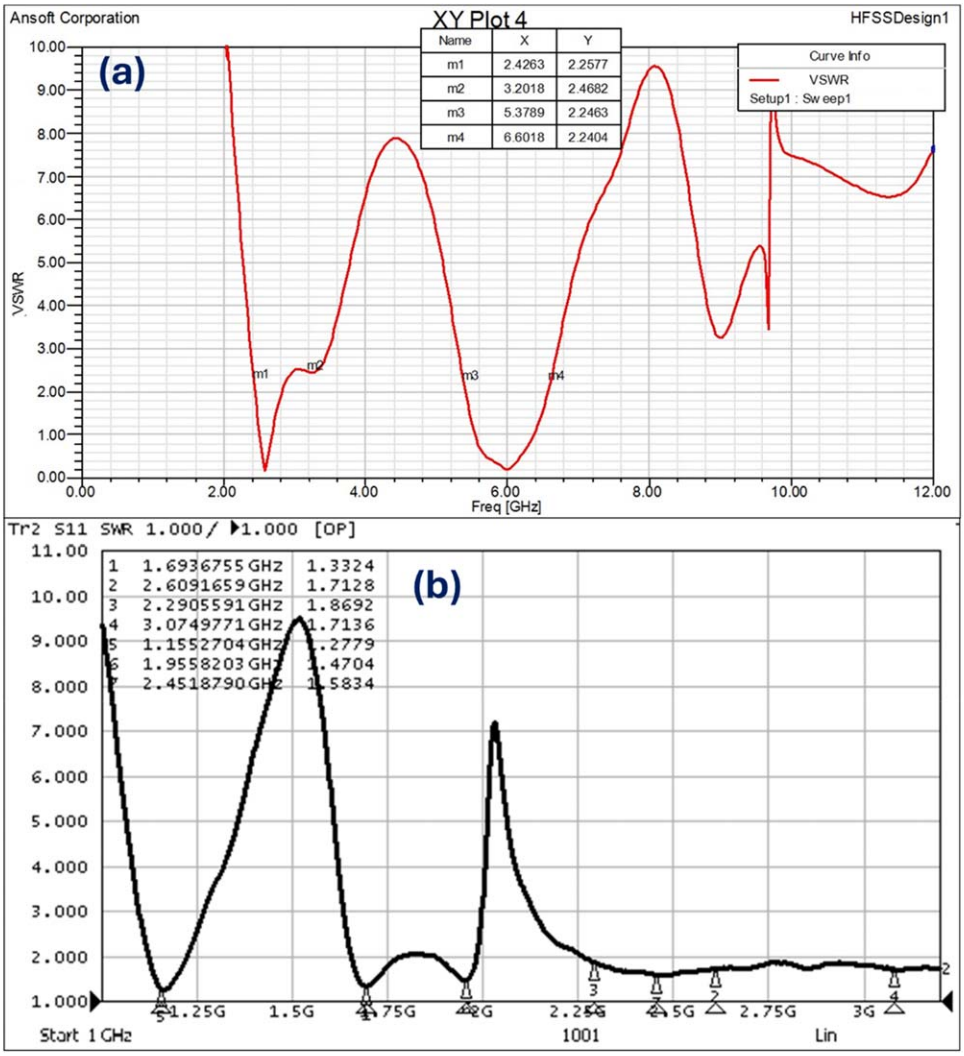

Figure 4. (a) VSWR of antenna—simulation results (b) VSWR of tested antenna- experimental results (Measurement limited to 1–3 GHz due to VNA range constraints).

alter the resonant characteristics. Second, the FR-4 substrate may exhibit non-uniform dielectric properties, especially at higher frequencies. Third, measurement setup effects, such as connector losses, cable radiation, and nearby metallic objects, can influence the VNA results. Despite these differences, the measured resonance bands closely follow the simulated trend, confirming the dual-band functionality and validating the proposed design's practical feasibility. Nevertheless, the experimental data substantiates the effective performance of the antenna within the intended frequency bands, particularly for applications in the S-band, showcasing the robustness and practical applicability of the proposed design.

It is important to note that the experimental VSWR measurements were constrained to the 1 GHz to 3 GHz range due to hardware limitations. Thus, only the S-band performance could be experimentally validated. The C-band functionality, confirmed by simulation, will be validated in future work using an extended-range vector network analyzer.

4.2. Reflection coefficient

The reflection coefficient measures the proportion of electromagnetic wave reflection occurring at an impedance discontinuity within the transmission channel. It represents the ratio of the reflected wave amplitude to the incident wave amplitude at the point of discontinuity [19]. A lower reflection coefficient signifies better impedance matching, enabling efficient power transfer and minimal signal loss. Return loss, expressed in positive decibels (dB), is calculated as $-20 \log_{10} |\Gamma|$, where Γ is the reflection coefficient and is used to evaluate the antenna's impedance-matching performance [20].

Figure 5 presents the reflection coefficient (S_{11}) of the proposed fractal MPA. The simulated graph (figure 5(a)) shows return loss dips below −10 dB at key frequencies—2.3244 GHz, 3.7692 GHz, 5.0936 GHz, and 7.1104 GHz—indicating effective impedance matching across the S-band and C-band ranges.

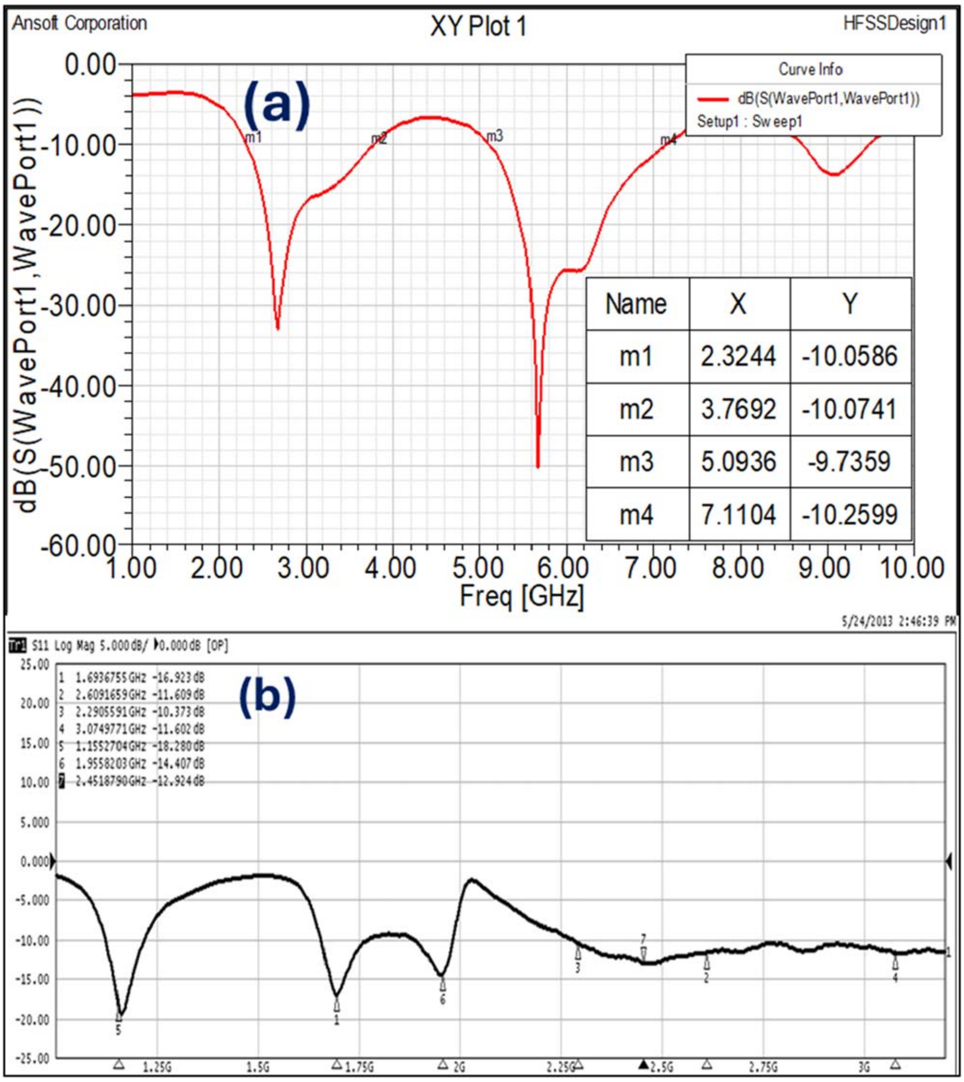

Figure 5. Simulated and measured reflection coefficient (S_{11}) of the proposed fractal MPA (a) Simulation results; (b) Experimental results (Measurement limited to 1–3 GHz due to VNA range constraints).

The measured graph (figure 5(b)), constrained to 1–3 GHz due to equipment limitations, shows good agreement in the S-band, validating the antenna's practical performance within the available testing range.

The return loss characteristics align closely with the VSWR results, validating the antenna's design and operational performance. The effective impedance matching demonstrated by the reflection coefficient confirms the antenna's capability for dual-band operation, making it suitable for applications in modern wireless communication systems within the S-band and C-band frequency ranges. The consistency between the simulated reflection coefficient and VSWR further underscores the robustness and reliability of the proposed antenna design.

The deviations in reflection coefficient between simulation and experiment can also be attributed to real-world effects not captured in simulation, such as contact impedance variation, copper surface roughness, and radiation from feeding lines. These lead to slight shifts in return loss values but do not significantly alter multiband performance, as both sets of results confirm operation within the targeted S-band and C-band frequency ranges.

As with the VSWR results, the reflection coefficient measurements were limited to frequencies below 3 GHz due to the measurement setup. The simulated C-band resonances remain untested in this work but are expected to align based on the consistency observed in the S-band. Extended frequency testing is planned for future studies.

4.3. Radiation Pattern

The radiation pattern of an antenna provides a graphical representation of its radiated energy distribution in space and is a crucial parameter for evaluating its directional behavior and efficiency [21]. Figure 6 illustrates the

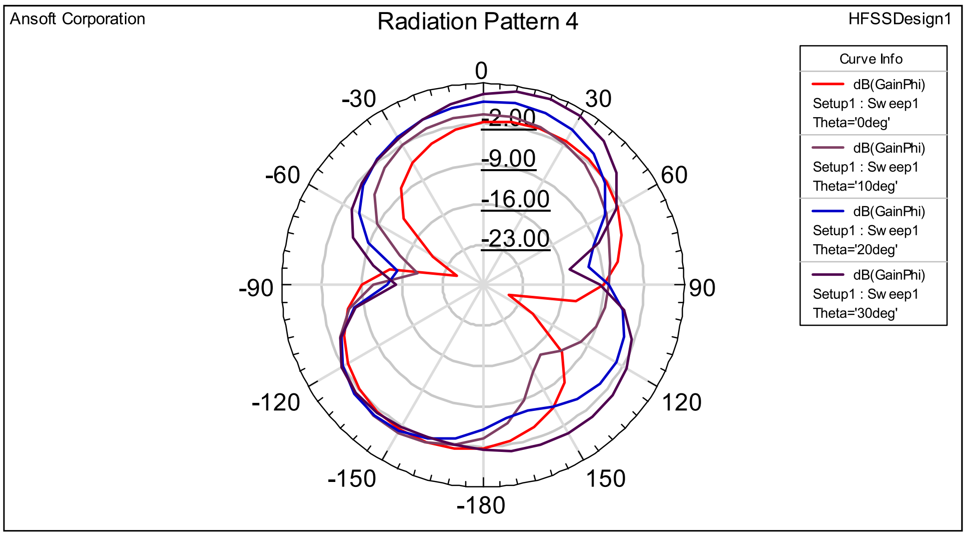

Figure 6. 2D E-Plane Radiation Pattern of the Antenna ($\phi = 0°$) at Elevation Angles $\theta = 0°$, $10°$, $20°$, and $30°$.

2D E-plane ($\phi = 0°$) radiation pattern of the proposed MPA at multiple elevation angles ($\theta = 0°$, $10°$, $20°$, and $30°$), demonstrating a characteristic bi-directional behavior with energy radiating in two opposite directions.

The pattern is plotted as a function of gain (in decibels) against the angular displacement (θ) from the reference plane, with measurements recorded at various elevation angles (e.g., $\theta = 0°$, $10°$, $20°$, and $30°$). The results highlight that the gain decreases as the angle deviates from the reference plane, indicating reduced radiation intensity at larger angular displacements. The symmetrical and nearly uniform distribution of the pattern underscores the consistency and stability of the antenna's performance, essential for reliable wireless communication. The bi-directional nature, evident from the 'figure-eight' shape, is advantageous for applications requiring focused coverage along a specific plane, such as point-to-point communication systems. These observations validate the antenna's design, showcasing its ability to achieve high directivity and controlled radiation characteristics. Combined with favorable VSWR and bandwidth performance, the radiation pattern analysis confirms the proposed antenna's suitability for modern multiband wireless communication systems, including WiMAX and 5G NR applications.

Figure 7 illustrates the 3D radiation patterns of the proposed MPA at various directions and frequency bands, specifically in the S-band of 2.2 GHz to 3.8 GHz and C-band of 5.02 GHz to 7.22 GHz. The patterns depict the spatial distribution of the radiated electromagnetic energy with color-coded intensity levels, where red indicates maximum radiation intensity and blue represents minimum radiation intensity.

Figure 7(a) highlights the omnidirectional nature of the antenna in one plane, with strong radiation observed along the Z-axis. Figure 7(b) provides a top-down view of the radiation pattern, demonstrating its symmetrical distribution and effective coverage. Figure 7(c) captures the cross-sectional view, highlighting the antenna's ability to maintain consistent radiation over a wide range of angles. Figure 7(d) showcases the pattern's doughnut-like shape, typical of patch antennas, with the null along the central axis and maximum radiation perpendicular to it. These patterns validate the antenna's design by demonstrating its ability to achieve efficient radiation and uniform coverage over the targeted frequency bands, making it suitable for modern wireless applications such as WiMAX and 5G NR. The observed radiation characteristics further confirm the effectiveness of fractal geometry in enhancing performance across multiple bands.

4.4. Smith chart

Figure 8 presents the Smith chart representation of the tested MPA, illustrating its simulation results across the operational frequency range. The Smith chart provides a comprehensive view of the antenna's impedance characteristics, which are essential for evaluating impedance matching and minimizing reflection losses. At 1.95 GHz, the antenna's impedance is approximately 51 Ω, closely aligning with the ideal value of 50 Ω. This indicates excellent impedance matching, ensuring minimal reflection and efficient power transfer between the antenna and the connected transmission line or RF circuitry. The trajectory on the Smith chart demonstrates stable impedance behavior across the frequency bands, with low reflection coefficients observed throughout. These results confirm the robustness of the antenna design in maintaining high performance and reliable operation across the targeted frequency bands.

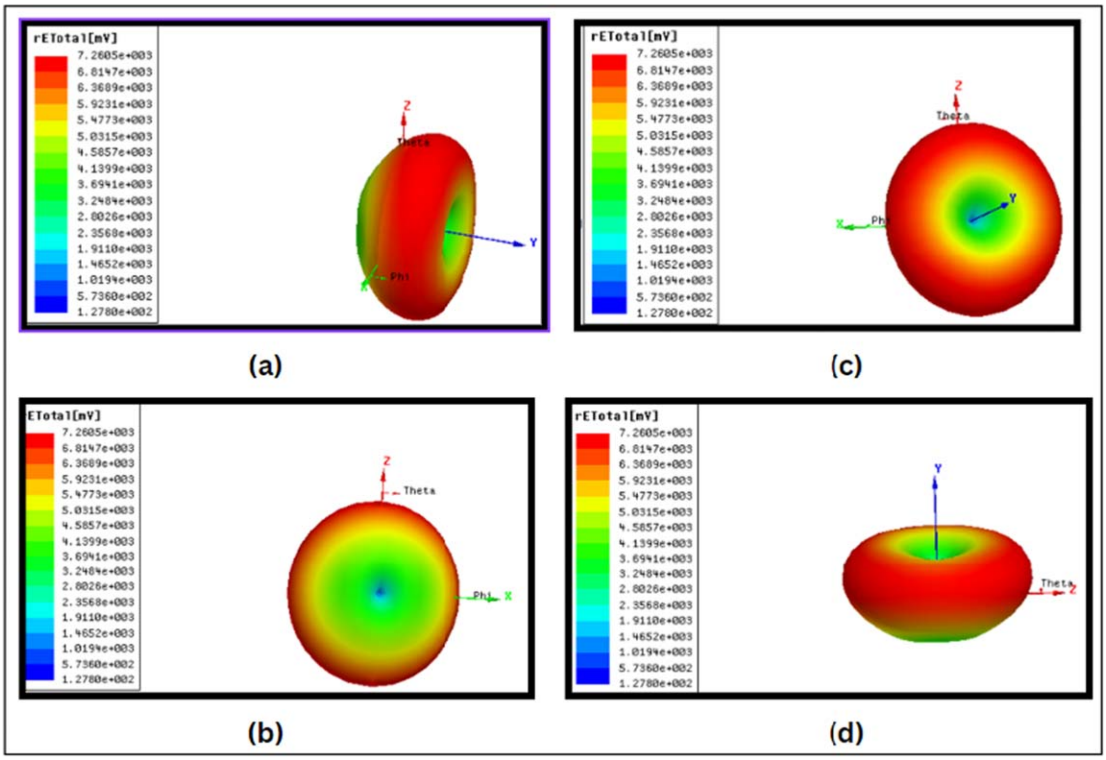

Figure 7. 3D radiation pattern of proposed antenna at various directions 2.2 GHz to 3.8 GHz and 5.02–7.22 GHz.

Figure 8(b) represents the experimental Smith chart of the tested MPA, showcasing its impedance characteristics across the operational frequency range from 1.6 GHz to 3.2 GHz. This chart is a vital tool for evaluating the antenna's impedance matching and reflection behavior. At 1.955 GHz, the impedance is approximately 51.80 Ω—j19.65 Ω, corresponding to a capacitive reactance of 4.14 pF, which is close to the ideal value of 50 Ω. This indicates good matching and efficient energy transfer at this frequency. Across other marked frequencies, the impedance values vary but remain within acceptable ranges, ensuring proper functionality across multiple bands. The loci on the Smith chart demonstrates low reflection coefficients around key frequencies, reflecting effective impedance matching and reduced standing wave ratio (SWR), which ensures efficient power delivery. The observed data shows a mix of inductive and capacitive reactances, as expected in practical multiband antennas, with variations effectively managed to showcase the design's robustness. Furthermore, the experimental results align closely with the simulated data, validating the design and fabrication processes. Minor discrepancies may be attributed to manufacturing tolerances, material properties, or measurement setup limitations. These findings confirm the proposed antenna's suitability for multiband wireless communication applications, supported by its stable impedance matching and strong radiation performance.

4.5. Current distribution

The surface current distribution of the proposed MPA plays a pivotal role in its radiation characteristics and overall performance [22]. Figure 9 presents the simulation results illustrating the surface current distribution in the antenna when power is supplied to the feed point. The plot highlights the variation in current density across the antenna surface, showing how the power is transferred from the feed point to the radiating elements. The distribution pattern provides insight into the antenna's performance, revealing the current flow and the resulting electromagnetic wave propagation characteristics. The simulation is carried out for frequency bands up to 8 GHz, showcasing a meticulous design demonstrating efficient results in VSWR, Smith Chart, and Reflection Coefficient analyses. The optimized current distribution minimizes energy losses, enhances radiation efficiency, and supports stable multiband operation, crucial for modern wireless communication systems.

Figure 10 illustrates the experimental setup used to measure the return loss and other parameters of the fabricated antennas using a Vector Network Analyzer (Planar 304/1). Multiple antenna prototypes are tested, with real-time results displayed on the connected PC for performance evaluation.

The simulation and fabricated results were validated and found to be in close agreement within the S-band, with minimal variations observed. The C-band performance (5.0–7.2 GHz) was only observed in simulations, as

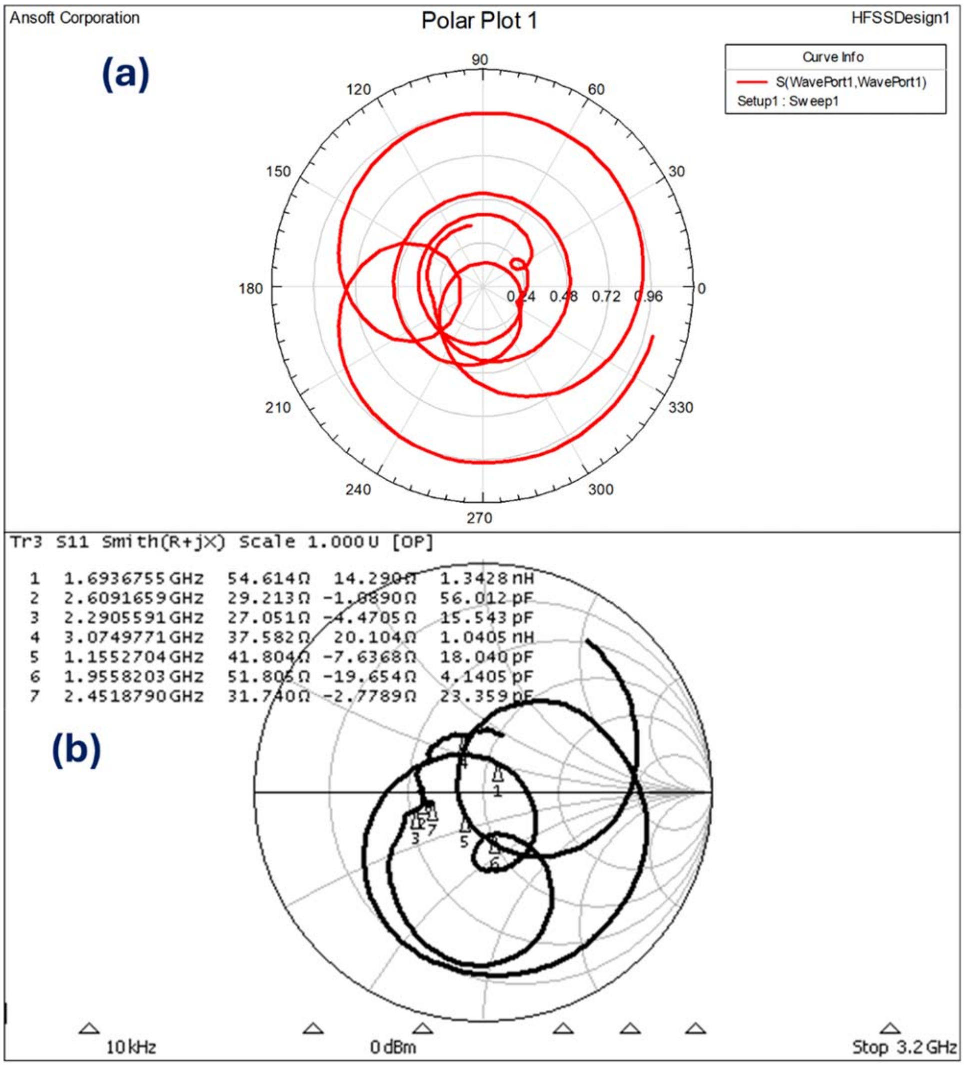

Figure 8. Smith chart of the tested antenna (a) simulation results; (b) experimental result (measurement limited to 1–3 GHz due to VNA range constraints).

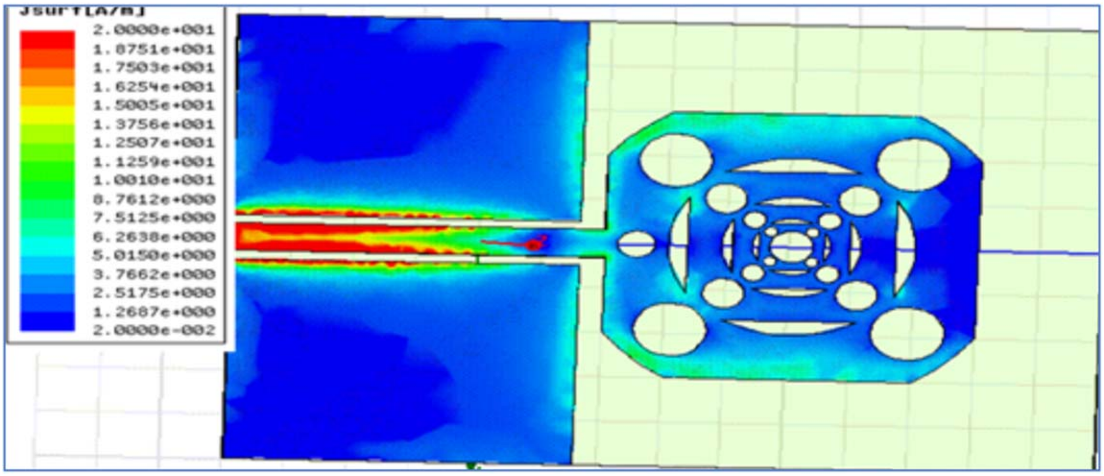

Figure 9. Simulation of surface current flow in the antenna with power supplied to the feed point.

the experimental measurement setup was restricted to the 1–3 GHz range. Comparative results are summarized in table 2, highlighting the simulated and measured frequencies for Return Loss, VSWR, and Smith Chart.

Figure 10. Antenna measurement setup using VNA.

Table 2. Comparison of results.

Applications	Simulated frequency	Measured frequency
Return loss	2.324 GHz–3.769 GHz 5.093 GHz–7.110 GHz	2.451 GHz–3.074 GHz
VSWR	2.294 GHz–3.824 GHz 5.378 GHz–7.230 GHz	2.290 GHz–3.074 GHz
Smith chart	2.242 GHz–3.829 GHz 5.02 GHz–7.22 GHz	2.290 GHz–3.074 GHz

These findings confirm the reliability and robustness of the proposed antenna design, making it suitable for applications such as WiMAX and 5G NR.

The slight discrepancies between the simulated and measured results are attributed to fabrication limitations, variation in FR-4 substrate properties, and experimental environment factors such as connector losses and external interference. However, the core performance indicators—VSWR <2 and return loss < -10 dB—are maintained, validating the antenna's efficacy. The close alignment in trend and operational band confirms the robustness of the proposed design.

The rising demand for patch antenna systems emphasizes the importance of designing antennas with characteristics tailored for specific applications [23]. While this study analyzed parameters such as VSWR, bandwidth, radiation pattern, peak gain, and efficiency, further improvements are needed to enhance these attributes across a broader frequency spectrum. Polarization and Radar cross-section (RCS) estimation, critical for applications in military and electronic warfare, were not addressed and should be considered in future studies to evaluate their impact on radiation properties [24]. Additionally, while this research utilized two patch elements as radiating components, exploring alternative methods for developing MPAs and conducting comparative analyses of their performance could help identify optimal designs for various applications.

While the proposed antenna utilizes a Coplanar Waveguide (CPW) feed, which is a type of microstrip line feed, table 3 presents a comparative analysis of common feeding techniques found in the literature. This table is included to highlight the design advantages of CPW-based feeding used in our work, especially in terms of minimizing spurious radiation and achieving wide bandwidth. A full comparative simulation and fabrication of all four feeding techniques is beyond the scope of this study but will be considered in future work for extended analysis.

Table 3 compares various microstrip antenna feeding techniques—including microstrip line, coaxial, aperture-coupled, and proximity-coupled feeds—across key performance parameters. The proposed design demonstrates minimum spurious radiation, reliable performance, and the highest bandwidth of 11%, emphasizing its novelty and suitability for modern wireless applications.

The proposed antenna is a Microstrip Fractal MPA designed to operate efficiently in WiMAX and 5G NR applications. Future research can aim to extend its functionality to emerging frequency bands, especially for high-speed applications in upcoming technologies like 5G and 6G. Enhancing polarization capabilities could expand its use in satellite communications and radar systems. Additionally, exploring various fractal geometries and leveraging advancements in material technologies can further improve performance in terms of size, efficiency, and bandwidth. Integrating cutting-edge concepts such as metamaterials or reconfigurable intelligent

Table 3. Comparative analysis of feeding techniques (literature-based) highlighting the benefits of the proposed CPW feed design.

Characteristics	Microstrip line feed	Coaxial feed	Aperture coupled feed	Proximity coupled feed	Novelty of the research
Spurious feed radiation	More	More	Less	Less	Minimum
Reliability	Better	Poor due to soldering	Good	Good	Good
Ease of fabrication	Easy	Soldering and drilling needed	Alignment required	Alignment required	Alignment required
Impedance matching	Easy	Easy	Easy	Easy	Easy
Bandwidth	2%–5%	2%–5%	2%–5%	9%	11%
Reference	[1, 3]	[8, 14]	[7, 17]	[9, 19]	**Our work**

surfaces (RIS) could enable adaptive behavior under varying environmental conditions. Investigating aspects like RCS reduction and low-profile designs for compact devices would also enhance its relevance for next-generation wireless networks. These directions open up new possibilities for creating more efficient, cost-effective, and versatile antenna systems for future all-wireless communication infrastructures.

5. Conclusion

The proposed Microstrip Fractal MPA has been successfully designed, simulated, fabricated, and experimentally tested for use in WiMAX and 5G NR applications. The antenna exhibits excellent performance across the targeted S-band and C-band frequency ranges, demonstrating low return loss, stable VSWR, and optimal impedance matching, which ensures minimal signal reflection and efficient power transfer. Radiation pattern analysis confirms a bi-directional profile, making the antenna well-suited for focused, point-to-point wireless communication. Also, Smith chart and surface current distribution analyses reveal robust impedance characteristics and efficient electromagnetic energy distribution. Experimental measurements align closely with simulation results, validating the reliability of the proposed design. A comparative evaluation with the initial square patch antenna further demonstrates that the proposed fractal structure achieves significant improvements in bandwidth, compactness, and multiband operation, validating the advantages of integrating fractal geometry and multi-slot design techniques. These features make the proposed antenna a promising candidate for compact, next-generation wireless systems. Future work could explore improvements in polarization control, RCS reduction, and high-frequency (e.g., 6G) compatibility, as well as the incorporation of emerging technologies such as metamaterials and reconfigurable surfaces to enhance adaptive performance.

Declarations

The authors declare the following statements related to conflicts of interest, data availability, funding, and author contributions.

Conflicts of interest

The authors declare that they have no known competing financial interests or personal relationships that could have appeared to influence the work reported in this paper.

Data availability

Data is provided within the manuscript.

Finding

This research did not receive any specific grant from funding agencies in the public, commercial, or not-for-profit sectors.

Author contributions

SAK wrote the original draft and contributed to conceptualization, data curation and methodology. **DDM** conducted an investigation, curated data, and reviewed and edited the manuscript. All authors reviewed the manuscript.

Data availability statement

All data that support the findings of this study are included within the article (and any supplementary files).

ORCID iDs

Dadaso D Mohite https://orcid.org/0000-0002-4296-1390

References

[1] Yogeshwaran A 2024 A multiple resonant microstrip patch heart shape antenna for satellite and Wi-Fi communication *Analog Integr Circ Sig Process* **121** 1–11
[2] Akkole S and Vasudevan N 2020 Design and optimization of E shape multi band microstrip patch antenna using fractal geometry for wireless communication *J. Comput Theor Nanosci* **17** 2409–14
[3] Wang L, Yu J, Xie T and Bi K 2021 A novel multiband fractal antenna for wireless application *International Journal of Antennas and Propagation* **2021** 1–9
[4] Abraham J and Mathew T 2015 Dual band david fractal microstrip patch antenna for GSM and WiMAX applications *WET* **06** 33–40
[5] Tilanthe P, Sharma P C and Bandopadhyay T K 2011 Gain enhancement of circular microstrip antenna for personal communication systems *IJET* **3** 175–8
[6] Alagarsamy M, Govindasamy S, Suriyan K, Rajangam B, Mariappan S and Krishnan J C R 2024 Performance analysis of microstrip patch antenna for wireless communication systems *IJRES* **13** 227
[7] Soni G K, Gour S and Sharma A 2021 Design and analysis of multi-band fractal antennas for wireless communications *Emerging Trends in Data Driven Computing and Communications* ed R Mathur *et al* (Springer) Studies in Autonomic, Data-driven and Industrial Computing 203–11
[8] Sharma N and Sharma V 2018 A design of microstrip patch antenna using hybrid fractal slot for wideband applications *Ain Shams Engineering Journal* **9** 2491–7
[9] Pravesh S, Nandana M K, Akshaya R and Christina Josephine Malathi A 2025 Study and design of heart-shaped microstrip patch antenna for SART applications *Results in Engineering* **25** 103819
[10] Saha D, Mandal S and Purkait K 2022 Design of rectangular slotted microstrip patch antenna for 5G applications at 27 GHz *2022 Int. Conf. on Intelligent Innovations in Engineering and Technology (ICIIET)* (IEEE) 15–9
[11] Kim G and Kim S 2021 Design and analysis of dual polarized broadband microstrip patch antenna for 5G mmWave antenna module on FR4 substrate *IEEE Access* **9** 64306–16
[12] Kaur A and Malik P K 2021 Multiband elliptical patch fractal and defected ground structures microstrip patch antenna for wireless applications *PIER B* **91** 157–73
[13] Kapoor A, Mishra R and Kumar P 2020 Compact wideband-printed antenna for sub-6 GHz fifth-generation applications *International Journal on Smart Sensing and Intelligent Systems* **13** 1–10
[14] Rashmi N, Raghavendra D, Vaidyanathan K and Akanksha A Design and implementation of multiband microstrip patch antenna for 5G-IOT communication system *2022 Sixth Int. Conf. on I-SMAC (IoT in Social, Mobile, Analytics and Cloud) (I-SMAC)* (IEEE) (2022) 88–93
[15] Ramaccia D *et al* 2022 Metasurface dome for above-the-horizon grating lobes reduction in 5G-NR systems *Antennas Wirel. Propag. Lett.* **21** 2176–80
[16] Nhlengethwa N L and Kumar P 2021 Fractal microstrip patch antennas for dual-band and triple-band wireless applications *International Journal on Smart Sensing and Intelligent Systems* **14** 1–9
[17] Al Ka'bi A 2022 Design of a microstrip dual band fractal antenna for mobile communications *2022 IEEE Int. Black Sea Conf. on Communications and Networking (BlackSeaCom)* (IEEE) 85–90
[18] Kadam S, Gurav S, Patil V, Jadhav P, Prabhakar A Y and Thorat H 2024 Design and performance of dual band microstrip nano-fractal patch antenna *Nano-Ntp* **20**
[19] Jeyapoornima B, Sheela J J J, Malarvizhi C, Vanaja S, Krishnan R and Atla R 2021 Multi-band narrow strip antenna for 5G/WLAN/WiMAX wireless communication *2021 Int. Conf. on Computer Communication and Informatics (ICCCI)* (IEEE) 1–4
[20] Hossain S, Rana M S and Rahman M M 2024 Design and analysis of inverted e-shaped slotted patch microstrip antenna for multiband applications *Data Engineering and Applications* 1189 ed J Agrawal *et al* in Lecture Notes in Electrical Engineering, vol. 1189 (Springer Nature Singapore) 385–99
[21] He Y, Lv S, Zhao L, Huang G-L, Chen X and Lin W 2021 A compact dual-band and dual-polarized millimeter-wave beam scanning antenna array for 5G mobile terminals *IEEE Access* **9** 109042–52
[22] Ajay V G, Parvathy A R and Mathew T 2019 Microstrip antenna with DGS based on CSRR array for WiMAX applications *IJECE* **9** 157
[23] Froumsia D, Jean-François E D, Houwe Kolyang A and Inc M 2022 Miniaturization of dual bands fractal-based microstrip patch fractal antenna for X and Ku bands applications *Eur. Phys. J. Plus* **137** 746
[24] Bhaldar H K *et al* 2023 Design of circular microstrip textile antenna for UWB application *IETE Journal of Research* **69** 5951–64